Received: 25 August 2023 | Revised: 12 January 2024 | Accepted: 15 February 2024

DOI: 10.1002/bit.28685

ARTICLE

BIOTECHNOLOGY AND BIOENGINEERING WILEY

Platform development for high-throughput optimization of perfusion processes—Part II: Variation of perfusion rate strategies in microwell plates

Marie Dorn[1] | Ciara Lucas[1] | Kerensa Klottrup-Rees[2] | Ken Lee[3] | Martina Micheletti[1]

[1]Advanced Centre for Biochemical Engineering, Department of Biochemical Engineering, University College London, London, UK

[2]Cell Culture and Fermentation Sciences, Biopharmaceutical Development, AstraZeneca, Cambridge, UK

[3]BioProcess Technologies and Engineering, Biopharmaceutical Development, AstraZeneca, Gaithersburg, Maryland, USA

Correspondence
Martina Micheletti, Advanced Centre for Biochemical Engineering, Department of Biochemical Engineering, University College London, Bernard Katz Bldg., Gower St., London WC1E 6BT, UK.
Email: m.micheletti@ucl.ac.uk

Funding information
AstraZeneca; Engineering and Physical Sciences Research Council; UK Engineering and Physical Sciences Research Council, Grant/Award Number: EP/S021868/1

Abstract

The biopharmaceutical industry is replacing fed-batch with perfusion processes to take advantage of reduced capital and operational costs due to the operation at high cell densities (HCD) and improved productivities. HCDs are achieved by cell retention and continuous medium exchange, which is often based on the cell-specific perfusion rate (CSPR). To obtain a cost-productive process the perfusion rate must be determined for each process individually. However, determining optimal operating conditions remain labor-intensive and time-consuming experiments, as investigations are performed in lab-scale perfusion bioreactors. Small-scale models such as microwell plates (MWPs) provide an option for screening multiple perfusion rates in parallel in a semi-perfusion mimic. This study investigated two perfusion rate strategies applied to the MWP platform operated in semi-perfusion. The CSPR-based perfusion rate strategy aimed to maintain multiple CSPR values throughout the cultivation and was compared to a cultivation with a perfusion rate of 1 RV d^{-1}. The cellular performance was investigated with the dual aim (i) to achieve HCD, when inoculating at conventional and HCDs, and (ii) to maintain HCDs, when applying an additional manual cell bleed. With both perfusion rate strategies viable cell concentrations up to 50×10^6 cells mL^{-1} were achieved and comparable results for key metabolites and antibody product titers were obtained. Furthermore, the combined application of cell bleed and CSPR-based medium exchange was successfully shown with similar results for growth, metabolites, and productivities, respectively, while reducing the medium consumption by up to 50% for HCD cultivations.

KEYWORDS
CSPR, high-throughput, microwell plate, perfusion, process development, small-scale

Abbreviations: Amm, ammonium; CCD, conventional cell density; CSPR, cell-specific perfusion rate; Glc, glucose; HCD, high cell density; HIP, high-intensity perfusion medium; Lac, lactate; mAb, monoclonal antibody; MWP, microwell plate; *q*, cell-specific production rate; RV, reactor volume; SF, shake flask; ST, spin tube; STY, space–time–yield; VCC, viable cell concentration.

1 | INTRODUCTION

Currently, the biopharmaceutical industry is shifting manufacturing processes from the well-established fed-batch to the more complex perfusion operation. This process intensification has the long-term goal of an end-to-end integrated continuous biomanufacturing process, connecting the upstream with the downstream process in a continuous fashion (Coolbaugh et al., 2021; Schwarz et al., 2022; Warikoo et al., 2012).

Perfusion has many advantages, although the continuous mode has a complex experimental set-up requiring additional pumps to achieve the continuous medium exchange and a cell retention device (Chotteau, 2015). In addition to its compatibility with an integrated process design, a perfusion operation can achieve very high cell densities (HCDs) due to the cell retention device, which in turn increases volumetric productivities and space–time–yields (STY). Furthermore, the continuous medium flow provides a constant metabolite supply to the cell culture as well as a continuous removal of impurities, which contributes to the low product residence times, resulting in consistent and improved product quality (Chotteau, 2015).

The continuous medium exchange is one of the main characteristics of a perfusion bioreactor as it generates stable process conditions avoiding the accumulation of unwanted and often toxic by-products while providing constant nutrient levels. The amount of exchanged medium is dependent on the perfusion rate and must be optimized for each cell line individually. Previously published studies report different ways to determine the perfusion rate, which can be based on the cell-specific perfusion rate (CSPR), the availability of the main substrate, the concentration of by-products, or a combination of these. The most common strategy used in previous studies is the determination of the perfusion rate based on the CSPR (Chotteau, 2015). It alters the perfusion rate proportionally to the viable cell concentration (VCC), thus resulting in a constant CSPR and metabolic environment over the cultivation time (Ozturk, 1996). Furthermore, a depletion of main substrates can be avoided while the accumulation of toxic by-products can be minimized providing that the cellular activities do not change over time or with VCC, thus allowing for HCD and consistent production to be achieved. The CSPR-based perfusion rate was successfully applied to manually and automatically controlled perfusion processes for the production of therapeutic proteins and virus-based biopharmaceuticals at bench-scale (Dowd et al., 2003; Gränicher et al., 2021; Nikolay et al., 2020; Vazquez-Ramirez et al., 2018) as well as in pilot and industrial scale (Coolbaugh et al., 2021; Konstantinov et al., 2006; Schwarz et al., 2022; Warikoo et al., 2012). To determine the CSPR with the highest productivity, different approaches can be used, such as the "push-to-low" approach (Konstantinov et al., 2006), a high-intensity, low-volume perfusion (HILVOP) process (Gagnon et al., 2018) or a combination of different cell concentrations and perfusion rates (Chotteau, 2015). Generally, lower CSPRs are preferred as this means more cells can be sustained with a certain amount of medium resulting in a reduction of the cost of goods manufactured (COGm). Furthermore, operations with CSPRs close to the minimum have been associated with higher productivities (Gagnon et al., 2018; Wolf & Morbidelli, 2020).

It is noteworthy that investigations of cellular performance at different perfusion rates are typically performed in lab-scale perfusion bioreactors. While scale-down models (SDMs) typically lack monitoring and control capabilities, they still are an interesting option for screening multiple CSPR-based perfusion rates before transferring the most promising conditions into a lab-scale perfusion bioreactor for more in-depth analysis and fine-tuning. Of particular interest are microwell plates (MWPs), as this platform allows for high-throughput and can be combined with automation, which enables the screening of several hundred conditions in parallel. Furthermore, the reduced format of operation contributes to higher experimental throughput and reduced costs in early development. This is especially advantageous during medium development, cell clone screening, and process development, where the MWP displays a straightforward and simple platform for practical handling and fabrication (Lindstrom & Andersson-Svahn, 2012). Previous studies showed that 24-well MWPs in semi-perfusion, using a total medium exchange once per day, can achieve growth to HCD and are a good representation of a 5 L perfusion bioreactor with a perfusion rate of 1 RV d^{-1} (Tregidgo et al., 2023). In this study, the MWP platform was evaluated for its ability to maintain different target CSPRs by changing the perfusion rate strategy from a fixed 1 RV d^{-1} to a CSPR-based regime. In particular, the influence of the CSPR-based perfusion rate strategy on achieving HCD was investigated when inoculating the MWPs at conventional (CCD) and high cell densities (HCD) and outcomes were compared with the cultivations using the established fixed medium exchange equivalent to a perfusion rate of 1 RV d^{-1}. In addition, investigations combining the CSPR-based perfusion rate strategy with the previously described cell bleed strategy were performed to evaluate the ability of the method to maintain HCD when using the CSPR-based perfusion rate strategy.

2 | MATERIALS AND METHODS

2.1 | Cell culture, cell line, and media

For all experiments, a Chinese hamster ovary (CHO) cell line, known as CHO cobra (Cobra Biologics AB), was used. The CHO cells were maintained in a perfusion-specific high-intensity perfusion (HIP) medium (Gibco®; Thermo Fisher Scientific), which was supplemented with 3.2 mM GlutaMax™-I (100X) (Gibco®; Thermo Fisher Scientific) and 2% 1X HT supplement (Gibco®; Thermo Fisher Scientific). During experiments, the medium was additionally supplemented with 30% CHO-CD EfficientFeed™ B (v/v) (Gibco®; Thermo Fisher Scientific).

The CHO cells were maintained in non-baffled shake flasks (Corning®) placed in a CO_2 incubator (MCO−19AIC; Sanyo) at 37°C with 5% CO_2. The shake flasks were agitated at a shaking speed of 180 rpm using an orbital shaking diameter of 25 mm (CO_2 resistant shaker; Thermo Fisher Scientific). Cells were passaged every 3–4 days and expanded into 2 L shake flasks for use in inoculation.

2.2 | Process operations

2.2.1 | Microwell plate cultivation

The procedure as previously described in Part I was used except for the inoculation. The MWPs (CLS3473; Corning®) were inoculated at 0.5–1 and 10–20 × 10^6 cells mL^{-1} with a working volume (V_W) of 1.2 mL for experiments targeting maximum growth and close to target VCC for experiments with an additional cell bleed strategy.

Samples were taken in triplicates using a sacrificial well methodology. If not otherwise indicated, samples were taken from "sampling wells" to determine VCC and viability, followed by a centrifugation step (50 g, 5 min). Postcentrifugation, supernatant was collected to quantify metabolites and titers, followed by a partial or total medium exchange in the "culture wells" to mimic perfusion with cell retention. Sampling and medium exchange were performed every 24 h over the duration of 8 days, where the day of inoculation marks day 0, if not otherwise indicated.

2.3 | Semiperfusion cultures with different medium exchange regimes

2.3.1 | Rigid RV d^{-1}-based exchange regime

The exchange regime based on the reactor volume per day (RV d^{-1}) describes a perfusion flow rate in terms of the total V_W. Thus, the perfusion rate is fixed (e.g., 1 RV d^{-1}) or can be increased stepwise (e.g., 1–1.5 to 2.0 RV d^{-1}).

2.3.2 | CSPR-based exchange regime

For the operation of CSPR-based semi-perfusion, it is assumed that the volume of exchange medium equals the amount of medium exchanged in a continuous perfusion process in the same time interval (Equation (1)). Thus, the exchange volume (V_E) is calculated based on V_W, a constant CSPR and the imminent VCC for a previously fixed schedule (Equation (2)). However, the schedule (Δt) is adapted when >60% of the V_W needs to be exchanged (Equation (3)).

$$Q_{\text{Perf}} = \frac{dV_E}{dt} = X_i \times V_W \times \text{CSPR} \times e^{\mu \Delta t}, \quad (1)$$

$$V_E = \frac{X_i}{\mu} \times (e^{\mu \Delta t} - 1) \times V_W \times \text{CSPR}, \quad (2)$$

$$\Delta t = \frac{\ln\left(\frac{0.6\mu}{X \times \text{CSPR}} + 1\right)}{\mu}, \quad (3)$$

where Q_{Perf} is the perfusion flow rate, CSPR is the cell-specific perfusion rate, μ is the specific growth rate, X_i is the average of three imminently measured viable cell concentrations, and Δt is the time between medium exchanges.

2.4 | Semi-perfusion culture with cell bleeds

The experimental procedure and calculations for the cell bleed strategy were described in Part I. The same procedure was applied for cultures using a CSPR-based medium exchange strategy. For cultures with a partial medium exchange, the previously removed bleed volume was taken into account for the removal of supernatant post centrifugation. In case the bleed volume exceeded the exchange volume ($V_B > V_E$), the bleed was collected in a separate sterile 50 mL centrifuge tube and centrifuged in parallel to the MWP. Supernatant from the bleed in the amount of $\Delta V_S = V_B - V_E$ was transferred back to the MWP before adding fresh medium equivalent to V_E to maintain a working volume of 1.2 mL.

2.5 | Analytics

The same analytical procedures as described in Part I were used. VCC and viabilities were determined using a ViCell™ XR cell viability analyzer (Beckman Coulter). Extracellular glucose, lactate, and ammonium concentrations were measured using an Optocell CuBiAn VC biochemistry analyzer (4BioCell), and product titers were determined using an HPLC (HPLC Agilent 1100 series; Agilent) with a 1 mL Protein G column (HiTrap™ Protein G HP; Cytiva).

For comparative analysis between different perfusion rate strategies, the following equations were used to determine cell-specific rates.

$$q = \left(\frac{\Delta c}{\Delta t \times \bar{X}}\right) + \frac{(H + B) \times c_i}{\bar{X}}, \quad (4)$$

where q is the cell-specific consumption/production rate, H is the daily harvest rate, B is the daily bleed rate, Δt is the time interval between two sampling time points, $\bar{X}$ is the daily average of the VCC, and c is the metabolite/product concentration.

To further evaluate the productivity between processes with varying conditions (i.e., perfusion flow rates) additional normalized parameters can be used as previously described by Bausch et al. (2019) for bioreactor operations. The space-time yield can be used to evaluate the overall productivity and is calculated using the following equations:

$$\text{STY} = \frac{Y_i}{V_W \times (t_i - t_0)}, \quad (5)$$

$$Y_i = \int_0^i c_{\text{mAb},i} \times H_i \times V_W \quad dt, \quad (6)$$

where STY is the space–time–yield, Y_i is the yield equal to the accumulated mass produced since the start of the cultivation, c_{mAb} is

the antibody concentration at time *i*, V_W is the working volume, *t* is the cultivation time, and *H* is the harvest rate.

3 | RESULTS

Perfusion processes aim to create a physiologically constant environment for the cells. In Part I, cell bleeds were performed to maintain a stable cell concentration, thus creating a quasi-steady state assuming a constant metabolic consumption. While this was achieved with a total medium exchange at a perfusion rate of 1 RV d^{-1}, Part II is focused on varying the perfusion rate with the aim of maintaining a stable CSPR at multiple setpoints. This CSPR-based perfusion rate results in partial medium exchanges, once or several times per day, to provide sufficient nutrients to support cell growth and production.

3.1 | Impact of seed concentration on growth, metabolic state, and productivity

Prior experimental investigation for this CHO cell line indicated a minimum CSPR of 13–15 pL $cell^{-1}$ d^{-1} (data not shown). Hence, the target CSPRs of 10, 15, and 20 pL $cell^{-1}$ d^{-1} were selected to perform the cultivation as close as possible to the minimum CSPR. The CSPR-based medium exchange strategy was investigated with two inoculation concentrations, as shown in Figure 1. The MWPs were inoculated at CCD between 0.5 and 2.0 × 10^6 cells mL^{-1} (Figure 1a) and at HCD between 10 and 20 × 10^6 cells mL^{-1}. For comparison, one (at CCD) or two (at HCD) MWPs with a perfusion rate equal to 1 RV d^{-1}, inoculated at CCD and HCD, respectively, were performed in parallel. In this work, the cultures with CSPR-based perfusion rate strategy are referred to as CSPR-cultures, where the targets of 10, 15, and 20 pL $cell^{-1}$ d^{-1} are also referred to as cultures with low, medium, and high CSPR targets, respectively. Furthermore, cultures with a perfusion rate of 1 RV d^{-1} are referred to as R1 and R2 for first and second runs, respectively.

As can be seen in Figure 1a, for the inoculation at CCD, all cultures performed equally in terms of cell growth, with viabilities above 95% over the entire cultivation period. After a short lag phase, cells started to grow exponentially reaching maximum values between 20.0 and 30.0 × 10^6 cells mL^{-1}. Interestingly, cultures with a perfusion rate strategy targeting 1 RV d^{-1} (total medium exchange) and a CSPR-based perfusion rate strategy targeting a CSPR of 20 pL $cell^{-1}$ d^{-1} (partial medium exchange) reached nearly identical maximum VCCs of 32.4 ± 1.5 × 10^6 cells mL^{-1} on day 8 and 31.1 ± 0.9 × 10^6 cells mL^{-1} on day 7, respectively. Furthermore, it was observed that VCCs of cultures with lower CSPR targets plateaued at VCCs around 23.0 × 10^6 cells mL^{-1} closely around their maximum VCC values. This suggests that for the cultures with low and medium CSPR targets (10 and 15 pL $cell^{-1}$ d^{-1}), the growth phase had turned from exponential to stationary, whereas a maximum VCC value was obtained at the end of the 8 days culture period for the culture with the high CSPR target. Hence, for the inoculation at HCD, this hypothesis was further investigated and growth, metabolic, and production performance was evaluated in the following.

As shown in Figure 1b, all cultures grew exponentially from the beginning. However, distinct differences can be observed between the R1 and R2 cultures following day 2, where R1 performed similarly to all cultures with CSPR-based perfusion rate strategy. From day 3 onwards, VCCs of R1 and CSPR-cultures plateaued at values around 40.0 × 10^6 cells mL^{-1} where low, medium, and high CSPR targets achieved a maximum at 46.6 ± 4.4, 44.4 ± 1.2, and 44.7 ± 1.8 × 10^6 cells mL^{-1}, respectively. R1 reached a maximum value of 43.5 ± 7.0 × 10^6 cells mL^{-1}. While CSPR-cultures maintained VCCs around 40.0 × 10^6 cells mL^{-1} until the end of cultivation, VCCs

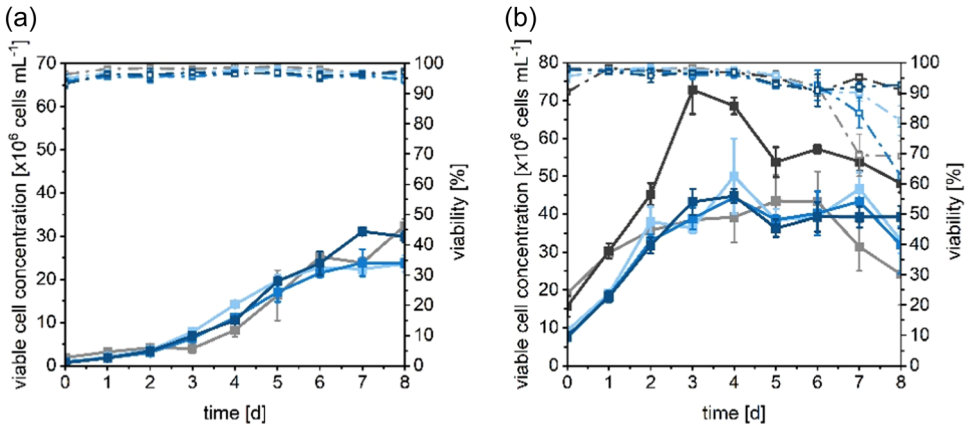

FIGURE 1 Cell growth for CHO cells in 24-well MWP cultivations in semi-perfusion with different perfusion rate strategies. Cells were cultivated in HIP medium supplemented with 30% Feed B (v/v). (a) Inoculation at 0.5–1 × 106 cells mL^{-1}. (b) Inoculation at 10–20 × 10^6 cells mL^{-1}. Growth (filled) and viability (open). Semi-perfusion was performed with a perfusion rate strategy based on CSPR targeting 10 (■), 15 (■), and 20 pL $cell^{-1}$ d^{-1} (■) and with a perfusion rate equal to 1 RV d^{-1}: R1 (■), R2 (■), where the R2 run was only performed at HCD inoculation. Mean of *N* = 3 wells. Error bars indicate standard deviation. CHO, Chinese hamster ovary; CSPR, cell-specific perfusion rate; HCD, high cell density; HIP, high-intensity perfusion medium; MWP, microwell plate.

of R1 decreased from day 6 to below 30.0×10^6 cells mL^{-1} on day 8. In contrast, R2 continued to grow to maximum values of around 70×10^6 cells mL^{-1} on days 3 and 4. Following this, the VCC rapidly dropped to values around 50.0×10^6 cells mL^{-1} and continued to decrease till the end. The viability remained above 95% for all cultures till day 4, followed by a decline. Viabilities of R1 and medium CSPR-cultures decreased below 70%, and low CSPR-cultures below 80% on day 8. R2 and high CSPR-cultures maintained viabilities above 90% until the end of the cultivation period. Overall, the cultures inoculated at HCD reached higher maximum VCCs as well as plateaued at higher VCC values, suggesting that the inoculation concentration has an impact on the maximum value of VCCs achievable in the culture.

The analysis of the external metabolites (glucose, lactate, and ammonium) showed similar dynamics between cultures run using different perfusion rate strategies (Figure 2). For simplicity, Figure 2 evaluates results of only one control culture for each inoculation concentration, where for HCD inoculation culture R2 with the higher maximum VCC was chosen. The result of similar dynamics was unexpected because of the varied nutrient supplies between the perfusion rate strategies. For glucose consumption, it was expected to see a sharper decline for CSPR-based cultures, as the medium exchange was only partial compared to a daily total medium exchange for the control culture. However, for CCD inoculation, glucose concentrations decreased continuously till day 8 (Figure 2a), where high CSPR-cultures had initially lower glucose concentrations than the rest of the cultures, but by day 5 concentrations were in a similar range. Despite R1 having the highest concentration at the end compared to medium and high CSPR-cultures, the concentrations were within the range of error. R1, medium and high CSPR-cultures maintained concentrations above 20 mmol L^{-1}, while low CSPR-cultures decreased to 12 mmol L^{-1} (Figure 2a). For HCD inoculation (Figure 2b), glucose concentrations achieved minimum values between 3 and 5 mmol L^{-1} on day 5 with no complete depletion for all cultures independent of the perfusion rate strategies used. An increase on day 8 was observed for all but the high CSPR-cultures, coinciding with the reduction in VCC (Figure 2b). The cell-specific glucose consumption rates (q_{Glc}, average over days 2–8) remained between 3.6 and 7.6 pmol cell^{-1} d^{-1} and 1.7–2.0 pmol cell^{-1} d^{-1} for CSPR-cultures at CCD and HCD concentration, respectively. Control cultures obtained q_{Glc} of 7.0 pmol cell^{-1} d^{-1} (R1 at CCD) and 1.3 pmol cell^{-1} d^{-1} for R2 at HCD.

Similarly, for lactate (Figure 2c,d) and ammonium concentrations (Figure 2e,f), it was expected to obtain higher values for cultures using the CSPR-based perfusion rate strategy as well as for cultures with HCD inoculation. As Figure 2c shows, lactate concentrations for cultures with CCD inoculation were in a similar range throughout the cultivation duration, with marginally higher concentrations for low and medium CSPR-cultures. Nonetheless, lactate concentrations remained around or below 15 mmol L^{-1}. For HCD inoculation cultures, lactate concentrations were, as expected, slightly higher than for CCD inoculation cultures and remained largely below 20 mmol L^{-1} for all conditions. The culture targeting a CSPR of 20 pL cell^{-1} d^{-1} reached higher concentrations than other CSPR-cultures. An increase in lactate concentrations for R2 and medium CSPR-cultures was observed on day 8. For CSPR-cultures, q_{Lac} remained between 1.3–2.3 pmol cell^{-1} d^{-1} and 0.4–0.6 pmol cell^{-1} d^{-1} for CCD and HCD inoculation concentration, respectively. Control cultures showed a q_{Lac} of 1.8 pmol cell^{-1} d^{-1} (R1 at CCD) and 0.3 pmol cell^{-1} d^{-1} for R2 at HCD.

While for the CCD inoculation, the ammonium concentration gradually increased, this concentration was in the same range for all conditions (Figure 2e). For the HCD inoculation, ammonium concentrations of CSPR-cultures were lower than for cultures using a total medium exchange. This was surprising as it was expected to see an accumulation of ammonium in CSPR-cultures (Figure 2f). However, for both CCD and HCD inoculations, ammonium concentrations remained well below 10 mmol L^{-1} and for the HCD inoculations all CSPR-cultures remained below 8 mmol L^{-1} (Figure 2e,f). For the CSPR-cultures, cell-specific ammonium production rates (q_{Amm}) remained between 0.6–1.0 pmol cell^{-1} d^{-1} and 0.2–0.3 pmol cell^{-1} d^{-1} for CCD and HCD inoculations, respectively. Control cultures obtained q_{Amm} of 1.0 (R1 at CCD) and 0.2 pmol cell^{-1} d^{-1} for R2 at HCD.

A hypothesis can be postulated for the similar metabolic behavior observed between cultures run using different perfusion rate strategies. Cultures using a CSPR-based perfusion rate are adapting to the partial medium exchanges by altering and potentially slowing down their metabolism, while cultures with RV d^{-1}-based perfusion rate experience more drastic changes in nutrient supply and toxic by-product removal which potentially enhance cell metabolism.

To compare the productivity between cultures at different conditions, normalized parameters such as the cell-specific production (q_p) or the space–time-yield (STY) are the most useful to evaluate the impact of operating conditions. In this work the perfusion rate strategies were varied, resulting in partial, instead of total, medium exchanges. Hence, for cultures with partial medium exchanges, the product concentration remaining in the culture must be considered. Figure 3a,b shows the cell-specific productivities for culture with CCD and HCD inoculations. For conditions inoculated at CCD, the q_p values of R1 cultures were lower in comparison to CSPR-cultures, and a significant difference (at the 5% level) was observed between the different perfusion rate strategies (Figure 3a). However, a slight reduction of q_p values was obtained with an increase in CSPR, and it was hypothesized that at similar CSPRs similar q_p values can be obtained. This hypothesis is supported by the results for cultures with HCD inoculation, where similar q_p values were obtained and no significant difference was observed (Figure 3b). The STY, shown in Figure 3c,d for the CCD and HCD inoculations, respectively, takes the different medium exchange volumes of the different perfusion rate strategies into account. It can be noted that for cultures with inoculation at CCD (Figure 3c), those with a CSPR-based perfusion rate strategy achieve higher STY on day 8, ranging between 0.1 and 0.15 g L^{-1} d^{-1}, whilst the STY for R1 remains below 0.05 g L^{-1} d^{-1}. For the experiments with inoculation at HCD, the STY obtained for R1 and R2 are higher compared to CSPR-cultures, achieving up to 0.7 g L^{-1} d^{-1} for R2 on day 8. However, the STY for R1 and high CSPR-cultures obtained were

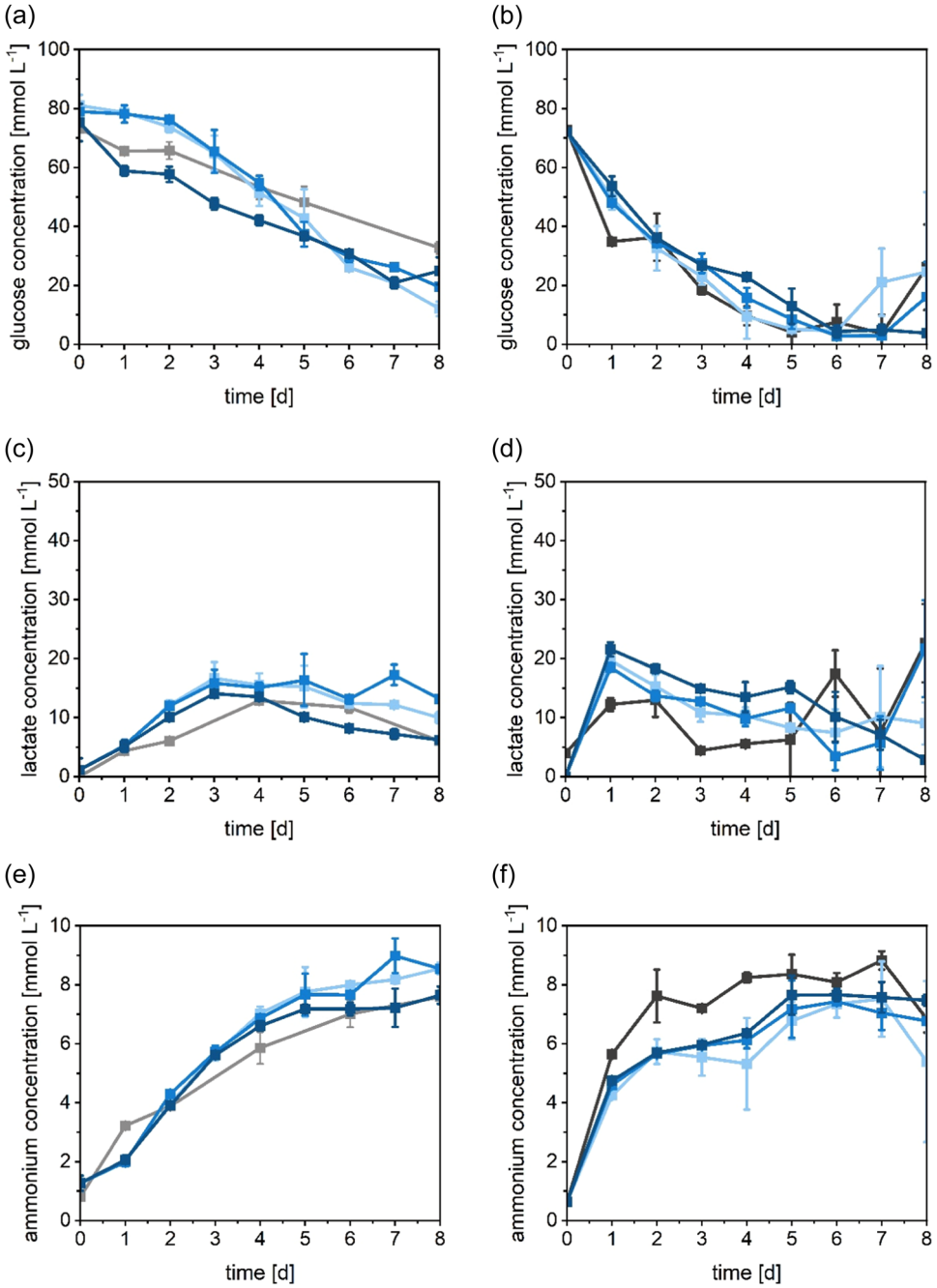

FIGURE 2 Metabolite concentrations for CHO cells in 24-well MWP cultivations in semi-perfusion with different perfusion rate strategies. Cells were inoculated at 0.5–1 × 10^6 cells mL^{-1} (a), (c), and (e) and at 10–20 × 10^6 cells mL^{-1} (b), (d), and (f) and cultivated in HIP medium supplemented with 30% Feed B (v/v). (a) and (b) Glucose concentration; (c) and (d) lactate concentration; (e) and (f) ammonium concentration. Semi-perfusion was performed with a perfusion rate strategy based on CSPR targeting 10 (■), 15 (■), and 20 pL $cell^{-1}$ d^{-1} (■) and with a perfusion rate equal to 1 RV d^{-1}: R1 (■), R2 (■), where the R2 run was only performed at HCD inoculation. Mean of $N = 3$ wells. Error bars indicate standard deviation. CHO, Chinese hamster ovary; CSPR, cell-specific perfusion rate; HCD, high cell density; HIP, high-intensity perfusion medium; MWP, microwell plate.

0.6 ± 0.1 and 0.5 ± 0.03 g L^{-1} d^{-1}, respectively, thus within the error range (Table 1). A comparison of the conditions targeting a CSPR of 20 pL $cell^{-1}$ d^{-1} with the control cultures R1 and R2 shows that similar maximum VCC, as well as similar productivities, could be obtained while the overall medium consumption was reduced by 65% for inoculation at CCD and by 23% for inoculation at HCD.

3.2 | Evaluation of process flow rates

In addition to the quantitative evaluation of the cell performance based on growth, metabolism, and mAb production data, it is crucial to analyze the perfusion rate and actual CSPR, as presented in Figure 4. While for the cultures R1 and R2 the perfusion rate was

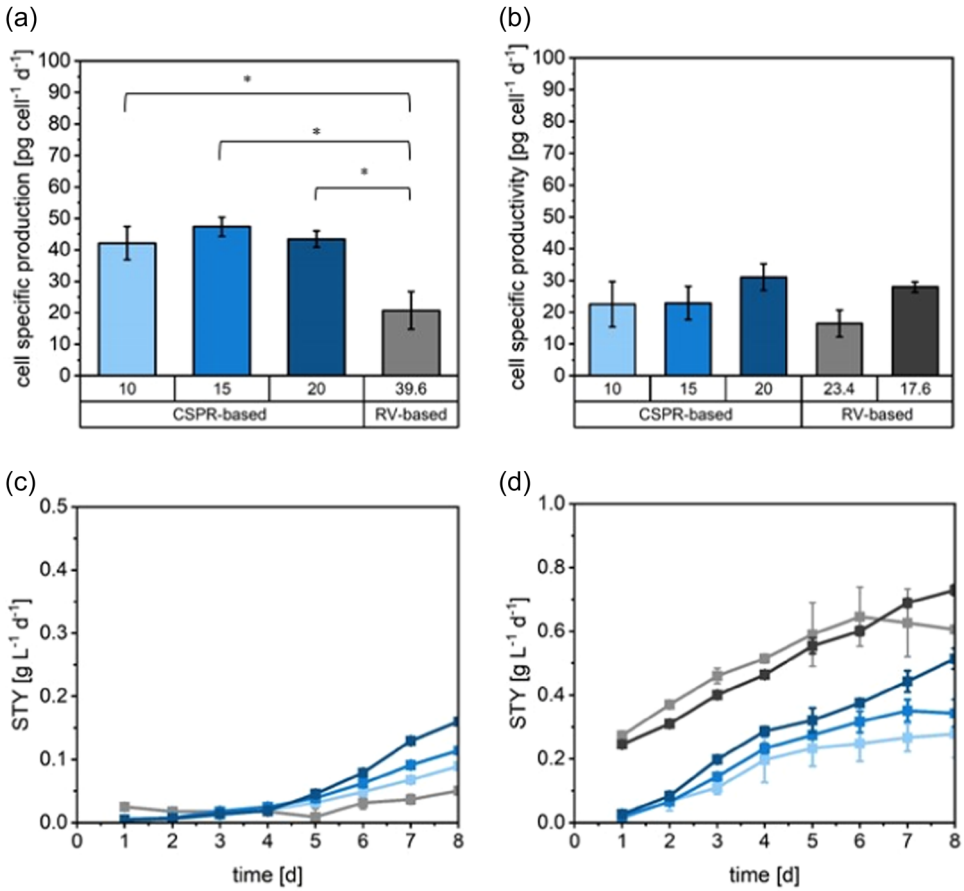

FIGURE 3 Cell-specific productivity for CHO cells in 24-well MWP cultivations in semi-perfusion with different perfusion rate strategies. Cells were inoculated at 0.5–1 × 106 cells mL^{-1} (a) and (c) and at 10–20 × 10^6 cells mL^{-1} (b) and (d) and cultivated in HIP medium supplemented with 30% Feed B (v/v). (a) and (b) Cell-specific production rate; (c) and (d) STY. Semi-perfusion was performed with a perfusion rate strategy based on CSPR targeting 10 (■), 15 (■), and 20 pL cell^{-1} d^{-1} (■) and with a perfusion rate equal to 1 RV d^{-1}: R1 (■), R2 (■), where the R2 run was only performed at HCD inoculation. Mean of $N = 3$ wells. Error bars indicate standard deviation. A t test analysis was used to evaluate significant difference for cell-specific mAb production rate between cultivation systems and VCC targets (*$p < 0.05$). CHO, Chinese hamster ovary; HCD, high cell density; HIP, high-intensity perfusion medium; mAb, monoclonal antibody; MWP, microwell plate; STY, space-time-yield; VCC, viable cell concentration.

TABLE 1 Process and cellular performance values for CHO cells in 24-well MWP culture comparing RV d^{-1} and CSPR-based perfusion rate strategies.

Inoculation	CCD				HCD				
Perfusion rate strategy	RV d^{-1}	CSPR			RV d^{-1}		CSPR		
CSPR target (pL cell^{-1} d^{-1})	R1	10	15	20	R1	R2	10	15	20
Average CSPR (pL cell^{-1} d^{-1})	39.6 ± 1.6[a]	10.4 ± 0.6	15.9 ± 1.4	21.1 ± 1.3	23.4 ± 3.5[a]	13.8 ± 1.2[a]	11.3 ± 0.8	16.8 ± 1.5	21.1 ± 1.5
Max. VCC (× 10^6 cells mL^{-1})	32.4 ± 1.5	23.7 ± 1.9	23.9 ± 3.0	31.1 ± 0.9	43.5 ± 6.9	72.9 ± 6.4	46.6 ± 4.4	44.4 ± 1.2	44.8 ± 1.8
STY (g L^{-1} d^{-1})[b]	0.03 ± 0.01	0.09 ± 0.00	0.09 ± 0.00	0.13 ± 0.00	0.61 ± 0.11	0.73 ± 0.02	0.28 ± 0.07	0.34 ± 0.04	0.51 ± 0.03
q_p (pg cell^{-1} d^{-1})	20.8 ± 5.9	42.1 ± 5.3	47.3 ± 3.0	43.4 ± 2.5	16.5 ± 4.2	27.9 ± 1.6	22.5 ± 7.1	22.8 ± 5.1	31.0 ± 4.1
V_M (mL)	129.6	39.8	42.9	44.7	129.6	129	66.2	82.4	99.8

Note: Cells were cultivated in high-intensity perfusion medium supplemented with 30% Feed B (v/v).

Yield and productivity values are given as average and standard deviation of $N = 3$ wells over the entire culture duration of 8 days.

Abbreviations: CCD, conventional cell density; CPO, Chinese hamster ovary; CSPR, cell-specific perfusion rate; HCD, high cell density; q_p, cell-specific productivity; RV, reactor volume; STY, space-time-yield; VCC, viable cell concentration; V_M, volume of consumed medium.

[a]Minimum value.

[b]Endpoint value on day 8.

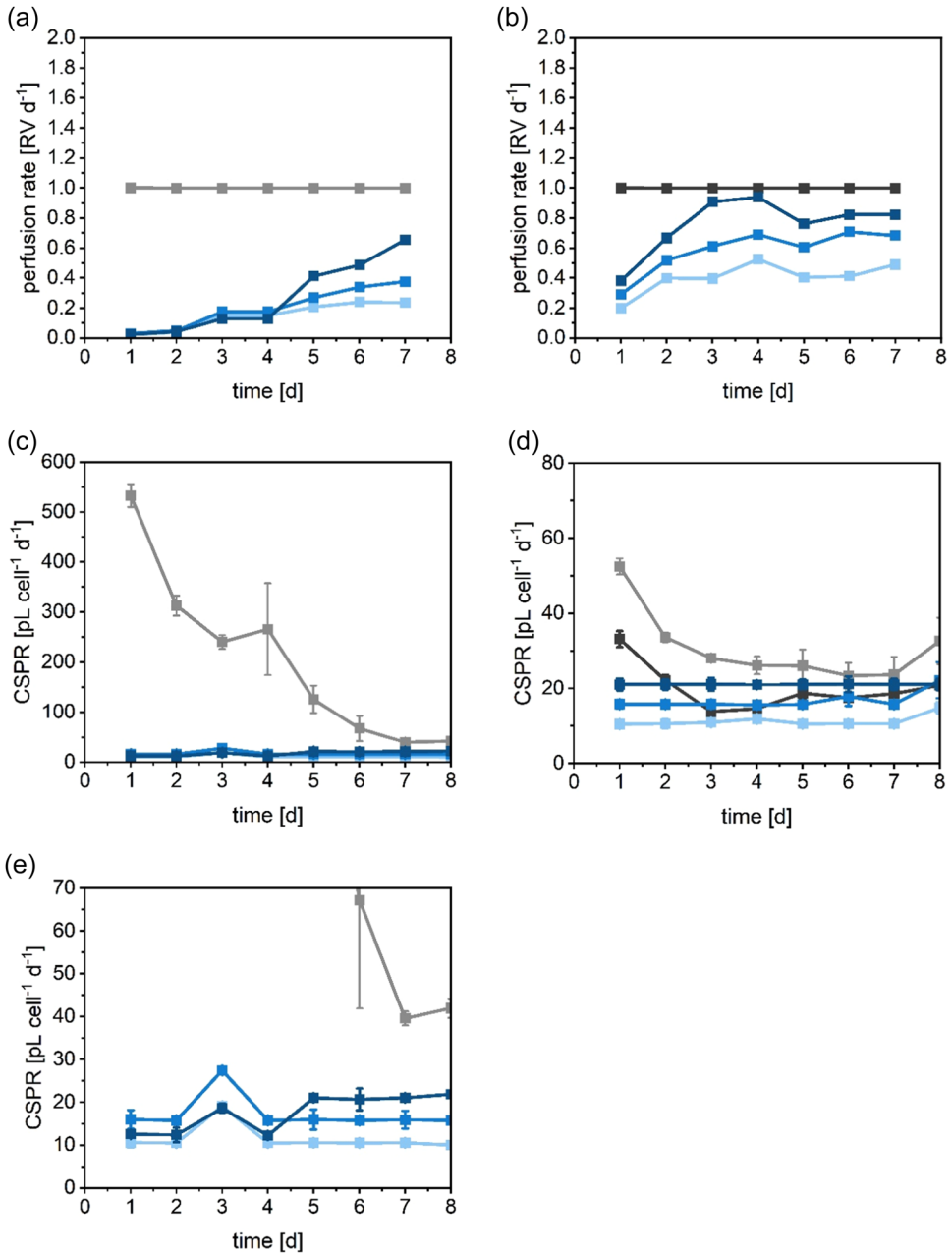

FIGURE 4 Process rates for CHO cells in 24-well MWP cultivations in semi-perfusion with different perfusion rate strategies. Cells were inoculated at 0.5–1 × 10^6 cells mL^{-1} (a), (c), and (e) and at 10–20 × 10^6 cells mL^{-1} (b) and (d) and cultivated in HIP medium supplemented with 30% Feed B (v/v). (a) and (b) Perfusion rate; (c) and (d) CSPR; (e) zoom of (c). Semi-perfusion was performed with a perfusion rate strategy based on CSPR targeting 10 (■), 15 (■), and 20 pL $cell^{-1}$ d^{-1} (■) and with a perfusion rate equal to 1 RV d^{-1}: R1 (■), R2 (■), where the R2 run was only performed at HCD inoculation. Mean of $N = 3$ wells. Error bars indicate standard deviation. CHO, Chinese hamster ovary; CSPR, cell-specific perfusion rate; HCD, high cell density; HIP, high-intensity perfusion medium; MWP, microwell plate.

constant (1 RV d^{-1}), for the CSPR-cultures, the perfusion rate is dependent on the cell growth. As expected, an increase in the perfusion rate was observed while the VCC increased for both CCD and HCD inoculation cultures (Figures 1 and 4a,b). Furthermore, higher perfusion rates were obtained at higher CSPR target values. For HCD inoculation cultures, it can be observed that the perfusion rate stabilized at different levels as soon as the VCCs plateaued (Figures 1 and 4b). The levels of stabilization depend on the target CSPR, and perfusion rates of around 0.5, 0.7, and 0.8 RV d^{-1} were obtained for cultures targeting a stable CSPR of 10, 15, and 20 pL $cell^{-1}$ d^{-1}, respectively.

The aim of this work was to keep the CSPRs stable for the duration of the culture, hence the actual CSPRs were analyzed for all CSPR cultures and compared to cultures using the RV d^{-1}-based perfusion rate strategy (Figure 4c–e). For CCD inoculation cultures, a significant difference in CSPRs was observed between the two

perfusion rate strategies. The total medium exchange of R1 cultures, with a perfusion rate equal to 1 RV d^{-1}, resulted in a decrease of CSPR from above 500 pL $cell^{-1}$ d^{-1} to minimum values of 40 pL $cell^{-1}$ d^{-1} on day 7 (Figure 4c), which is well above the target CSPRs for CSPR-cultures (Figure 4c,e). Using the CSPR-based perfusion rate strategy it was possible to keep CSPRs low and around the target. In the first days of cultivation using the CSPR-based perfusion rate strategy, the actual CSPRs were initially lower and fluctuated around the target. However, from day 4 the target CSPR could be maintained, resulting in average CSPRs of 10.3 ± 0.6, 15.9 ± 1.4, and 21.1 ± 1.3 pL $cell^{-1}$ d^{-1} over the last 4 days of culture for the target of 10, 15, and 20 pL $cell^{-1}$ d^{-1}, respectively (Figure 4e and Table 1). Smaller differences in CSPRs were found for cultures inoculated at HCD (Figure 4d). Similarly, to what was previously observed, the CSPRs of R1 and R2 initially declined and then stabilized from day 3 at values around 25 and 20 pL $cell^{-1}$ d^{-1} for R1 and R2, respectively. A slight increase of CSPRs was observed for R1 and R2 on day 8. Both the stabilization of CSPRs and the slight increase observed at the end of the culture align with the VCC dynamic trend observed in Figure 4d. In contrast to this, the actual CSPRs of cultures using the CSPR-based perfusion rate strategy were maintained throughout the cultivation duration with average values of 11.3 ± 0.8, 16.8 ± 1.5, and 21.1 ± 1.5 pL $cell^{-1}$ d^{-1} for the targets of 10, 15, and 20 pL $cell^{-1}$ d^{-1}, respectively (Figure 4d and Table 1).

Overall, a total medium volume of 129 mL per plate was utilized by cultures at a perfusion rate equal to 1 RV d^{-1}. Cultures run using the CSPR-based perfusion rate strategy utilized 40, 43, and 45 mL, for inoculation at CCD, and 67, 83, and 100 mL, for inoculation at HCD, for the targets of 10, 15, and 20 pL $cell^{-1}$ d^{-1}, respectively. This accounts for a reduction of medium consumption by up to 70% for low and up to 50% for high seeding densities experiments.

3.3 | Integration of CSPR-based perfusion rate and cell bleed strategy

Following the successful application of the CSPR-based perfusion rate strategy to conditions targeting maximum growth and the stabilization of VCCs for cultures inoculated at HCD, this perfusion rate strategy was combined with the cell bleed strategy implemented and discussed in Part I. The aim of the experiment was to maintain a stable average VCC of 20×10^6 cells mL^{-1} while maintaining three different CSPR targets. As observed in the previous investigation (Section 3.1), cultures targeting a CSPR of 15 and 20 pL $cell^{-1}$ d^{-1} showed very good performance in terms of growth and productivity, therefore these two CSPR conditions were selected for in-depth investigations. A third target CSPR of 30 pL $cell^{-1}$ d^{-1} was also included, hereafter referred to as "very high CSPR." This value was selected as it was the average CSPR obtained for cultures targeting a stable VCC of 20×10^6 cells mL^{-1} using a perfusion rate equal to 1 RV d^{-1}, as previously shown in Part I. For comparison, a cultivation with a perfusion rate equal to 1 RV d^{-1} was performed in parallel.

Figure 5 shows the cell growth and the CSPR variation with culture time. For all conditions, the typical "saw-wave"-like oscillation around the target average VCC was obtained (Figure 5a). This profile was maintained for the control culture throughout the cultivation, obtaining an average VCC of $23.8 \pm 1.5 \times 10^6$ cells mL^{-1}, while cultures with a CSPR-based medium exchange showed larger fluctuations above and below the mean value commencing on day 3 (Figure 5a). Nevertheless, average VCC values of 20.7 ± 1.7, 21.4 ± 1.9, and $21.6 \pm 2.4 \times 10^6$ cells mL^{-1} were obtained with perfusion rates aimed at constant CSPRs of 15, 20, and 30 pL $cell^{-1}$ d^{-1}, respectively (Table 2). Overall, the viabilities remained above 90% with a minor decline towards the end of the cultivation (Figure 5a).

Analyzing the actual CSPR values showed, however, that these were initially below the target and could only be maintained constant over time for the medium and high CSPR targets of 15 and 20 pL $cell^{-1}$ d^{-1} (Figure 5b). The actual CSPRs of cultures targeting a constant value of 30 pL $cell^{-1}$ d^{-1} remained below the target but increased over the cultivation duration. Overall average CSPRs of 14.5 ± 0.9, 17.6 ± 1.4, and 24.3 ± 2.1 pL $cell^{-1}$ d^{-1} were obtained for medium, high, and very high CSPR targets (Table 2). The control culture showed an initial decrease of the CSPR value before stabilizing around 23 pL $cell^{-1}$ d^{-1} between days 2 and 6, to then increase towards the end of culture (Figure 5b and Table 2).

Process flow rates remained largely stable over the process duration (cf. Figure 5c,d). The perfusion rates showed minor fluctuations over time and were stable throughout at different levels, with average values of 0.6, 0.7, and 0.9 RV d^{-1} for CSPR targets of 15, 20, and 30 pL $cell^{-1}$ d^{-1}. Hence, for all CSPR-based cultures, the perfusion rate was on average below that of the control cultures (Figure 5c, Table 2). The bleed rates, shown in Figure 5d, showed large fluctuations for all conditions when a CSPR-based medium exchange was used; however, it remained between 0.2 and 0.3 RV d^{-1} and slightly below the bleed rates of the control culture at around 0.4 RV d^{-1}. The larger fluctuations of bleed rates correspond to the differences observed between the different perfusion rate strategies, in particular lower growth in CSPR than control cultures.

The analysis of the external metabolites, glucose and lactate, is shown in Figure 6a,b. For all conditions similar metabolic dynamics were obtained, in particular stable glucose and lactate concentrations were observed after day 1 (Figure 6). As expected, the glucose concentrations for cultures targeting lower CSPRs were the lowest values, where cultures aiming at a CSPR of 15 and 20 pL $cell^{-1}$ d^{-1} obtained average values of 23.1 ± 1.5 and 25.2 ± 0.9 mmol L^{-1} (q_{Glc}: 1.16 and 1.35 pmol $cell^{-1}$ d^{-1}), respectively (Figure 6a and Table 2). Cultures with a perfusion rate strategy aiming at a stable CSPR of 30 pL $cell^{-1}$ d^{-1} and cultures with a perfusion rate equal to 1 RV d^{-1} showed similar glucose concentration levels at 32.6 ± 2.0 and 28.7 ± 1.5 mmol L^{-1} (q_{Glc}: 1.70 and 2.20 pmol $cell^{-1}$ d^{-1}), respectively (Table 2). Furthermore, an increase in glucose concentration from day 6 was observed for both conditions. These similarities are in agreement with the results observed from monitoring the actual CSPR obtained from both cultures showing very similar dynamics.

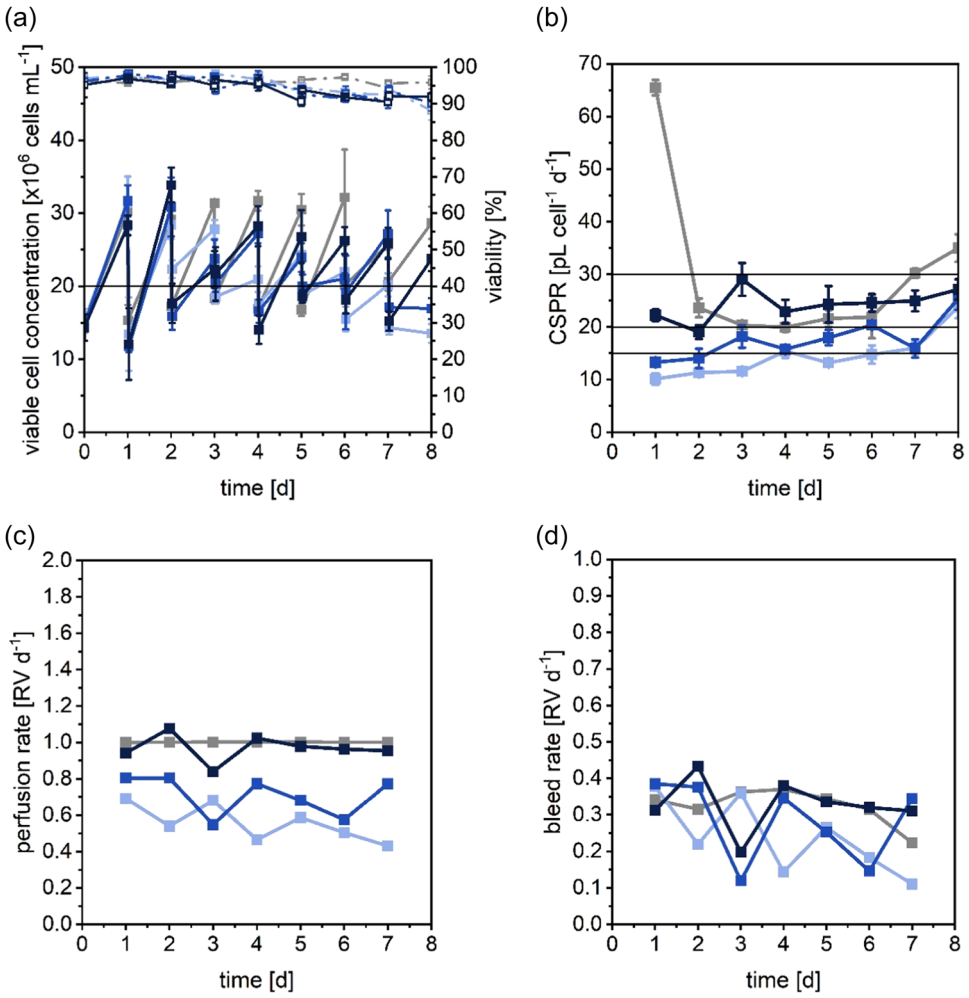

FIGURE 5 Viable cell concentrations, cell-specific perfusion rates, and bleed rates for CHO cells in 24-well MWP cultivations in semi-perfusion with implemented cell bleeds. Cells were inoculated at 10, 20, 30, and 40 × 10^6 cells mL^{-1} and cultivated in HIP medium supplemented with 30% Feed B (v/v). (a) Growth (filled) and viability (open); (b) cell-specific perfusion rate (CSPR); (c) perfusion rate; (d) bleed rate. Targeted CSPRs (× 10^6 cells mL^{-1}): 15 (■), 20 (■), 30 (■). Perfusion rate equal to 1 RV d^{-1} (■). Mean of $N = 3$ wells. Error bars indicate standard deviation. CHO, Chinese hamster ovary; MWP, microwell plate.

The comparable CSPR dynamic and glucose consumptions are an indicator of an overall similar metabolic behavior between the two conditions at different medium exchange regimes. For lactate concentration, it was expected to see larger values for cultures targeting a lower CSPR, where the smaller exchange volume leads to an accumulation of lactate. However, the lowest lactate concentrations were observed for the cultures with a perfusion rate strategy targeting 15 and 20 pL $cell^{-1}$ d^{-1}, with average values of 9.0 ± 0.5, 10.6 ± 0.4, and 12.2 ± 0.6 mmol L^{-1} (q_{Lac}: 0.23, 0.34, 0.53 pmol $cell^{-1}$ d^{-1}) for the cultures targeting a stable CSPR of 15, 20, and 30 pL $cell^{-1}$ d^{-1}, respectively (Figure 6b and Table 2). The control culture with a total medium exchange showed stable lactate concentrations of 11.6 ± 1.0 mmol L^{-1} (q_{Lac}: 0.46 pmol $cell^{-1}$ d^{-1}). Ammonium concentrations stabilized after day 1 with values below 10 mmol L^{-1} for all conditions (q_{Amm} < 0.29 pmol $cell^{-1}$ d^{-1}) (Table 2).

The STY and cell-specific productivity were calculated and are presented in Figure 7. For all conditions, and independent of the perfusion rate strategy, similar dynamics for STY (Figure 7a) and q_p (Figure 7b) were obtained. For all conditions, the STY initially increased before stabilizing at around 0.2 g L^{-1} d^{-1}. The CSPR-cultures targeting a CSPR of 30 pL $cell^{-1}$ d^{-1} achieved 0.18 g L^{-1} d^{-1} on day 8, which is equivalent to the value obtained for cultures using a total medium exchange (Figure 7a and Table 2). Although the cell-specific productivities of CSPR-cultures are slightly higher than control cultures, no significant difference was observed. For CSPR-cultures, a value of q_p around 36.0 pg $cell^{-1}$ d^{-1} was achieved, whereas for the control culture, the q_p values was equal to 24.5 ± 1.4 pg $cell^{-1}$ d^{-1} (Figure 7b and Table 2).

Overall, the total medium volume of 129 mL per plate, utilized for a culture using a perfusion rate of 1 RV d^{-1}, was reduced to 61, 72, and 92 mL for cultures with a CSPR-based perfusion rate strategy with CSPR targets of 15, 20, and 30 pL $cell^{-1}$ d^{-1}, respectively. This accounts for a reduction of medium consumption of up to 53%.

TABLE 2 Steady-state values for CHO cells in 24-well MWP culture with implemented cell bleed and with different perfusion rate strategies targeting an average value of 20×10^6 cells mL^{-1}.

Perfusion rate strategy	RV d^{-1}	CSPR		
CSPR target (pL $cell^{-1}$ d^{-1})	R1	15	20	30
Average VCC ($\times 10^6$ cells mL^{-1})	23.8 ± 1.5	20.7 ± 1.7	21.4 ± 1.9	21.6 ± 2.4
Metabolites				
Glc (mmol L^{-1})	28.7 ± 1.5	23.1 ± 1.5	25.2 ± 0.2	32.6 ± 1.9
Lac (mmol L^{-1})	11.6 ± 1.0	9.0 ± 0.5	10.6 ± 0.4	12.2 ± 0.6
Amm (mmol L^{-1})	6.2 ± 0.2	6.0 ± 0.2	6.6 ± 0.1	6.6 ± 0.2
Productivity				
STY [g L^{-1} d^{-1}][a]	0.18 ± 0.00	0.12 ± 0.00	0.15 ± 0.00	0.18 ± 0.01
q_p (pg $cell^{-1}$ d^{-1})	24.6 ± 1.4	38.4 ± 2.6	37.9 ± 1.8	31.0 ± 4.2
Flow rates				
Perfusion (RV d^{-1})	1.00	0.56	0.71	0.97
Harvest (RV d^{-1})	0.75	0.32	0.43	0.64
Bleed (RV d^{-1})	0.35	0.24	0.28	0.33
Average CSPR (pL $cell^{-1}$ d^{-1})	24.7 ± 1.7	14.5 ± 1.0	17.6 ± 1.4	24.3 ± 2.1
V_M (mL)	129.6	60.5	71.1	92.2

Note: Cells were cultivated in HIP medium supplemented with 30% Feed B (v/v).

Yield and productivity values are given as average and standard deviation of $N = 3$ wells over the entire culture duration of 8 days.

Abbreviations: Amm, Ammonium; CSPR, cell-specific perfusion rate; Glc, glucose; Lac, lactate; RV, reactor volume; STY, space–time–yield; q_p, cell-specific productivity; VCC, viable cell concentration; V_M, volume of consumed medium.

[a]Endpoint value on day 8.

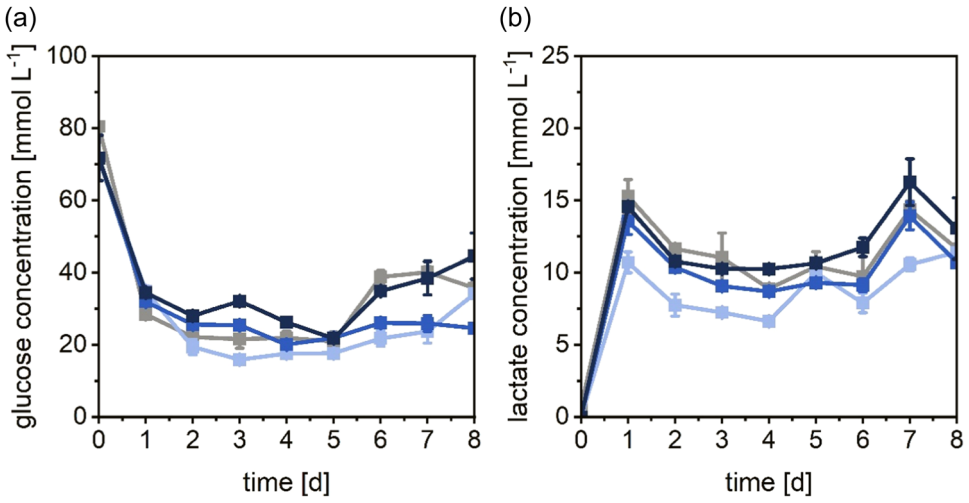

FIGURE 6 Metabolite concentrations for CHO cells in 24-well microwell plate cultivations in semi-perfusion with implemented cell bleeds. Cells were inoculated at 20×10^6 cells mL^{-1} and cultivated in HIP medium supplemented with 30% Feed B (v/v). (a) Glucose concentration; (b) lactate concentration. Targeted CSPRs ($\times 10^6$ cells mL^{-1}): 15 (■), 20 (■), 30 (■). Perfusion rate equal to 1 RV d^{-1} (■). Mean of $N = 3$ wells. Error bars indicate standard deviation. CHO, Chinese hamster ovary; CSPR, cell-specific perfusion rate; HIP, high-intensity perfusion medium.

4 | DISCUSSION

In this work, two perfusion rate strategies, RV d^{-1}-based or CSPR-based, were implemented in a small volume platform for the first time and their impact on cell growth, productivity, and metabolic performance were investigated to evaluate their applicability and feasibility for robust cell clone screening operations. To the best of our knowledge, non-instrumented small-scale models in semi-perfusion have only been operated with a fixed RV d^{-1}-based perfusion rate strategy in the published literature, resulting in a

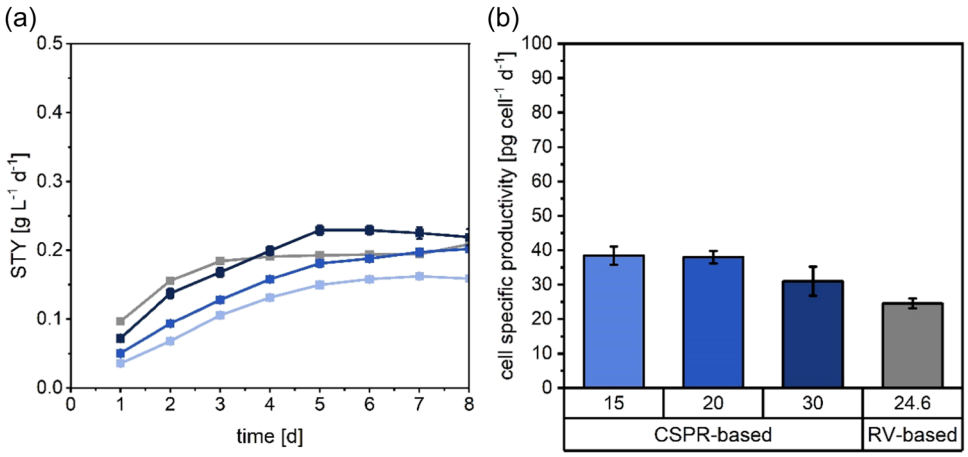

FIGURE 7 Productivities for CHO cells in 24-well microwell plate cultivations in semi-perfusion with implemented cell bleeds. Cells were inoculated at 20×10^6 cells mL^{-1} and cultivated in HIP medium supplemented with 30% Feed B (v/v). (a) STY; (b) q_p. Targeted CSPRs ($\times 10^6$ cells mL^{-1}): 15 (■), 20 (■), 30 (■). Perfusion rate equal to 1 RV d^{-1} (■). Mean of $N = 3$ wells. Error bars indicate standard deviation. CHO, Chinese hamster ovary; CSPR, cell-specific perfusion rate; HIP, high-intensity perfusion medium; STY, space-time-yield.

manual medium exchange once or twice per day (Mayrhofer et al., 2021; Tregidgo et al., 2023; Villiger-Oberbek et al., 2015; Wolf et al., 2018). However, the RV d^{-1}-based strategy does not consider the actual state of the cell culture. This might result in under- or oversupply of metabolites and accumulation of inhibitory by-products, thus significantly impacting cell growth and productivities (Karst et al., 2017; Nikolay et al., 2020). In contrast, the CSPR-based perfusion rate strategy takes the current state of the cell culture into account by considering the VCC at the time of sampling and resulting in a partial medium exchange. Providing that cellular activity does not change, the CSPR and the medium composition can be kept constant allowing for consistent production (Chotteau, 2015; Ozturk, 1996).

4.1 | Application of two different perfusion rate strategies during maximum growth conditions

Firstly, the two perfusion rate strategies (RV d^{-1}-based or CSPR-based) were applied with the aim to achieve maximum viable cell concentrations and experiments were performed for two different inoculation concentrations, at CCD and HCD. For both cases, the results obtained for growth and metabolism were comparable between all CSPR targets, for the CSPR-based strategy and the RV d^{-1}-based strategy. An exception was the R2 culture using the RV d^{-1}-based strategy at HCD inoculation, which obtained maximum VCCs 1.6-fold higher than R1, as well as all cultivations using a perfusion rate strategy based on CSPR. Opposite to the CSPR-cultures, the R1 and R2 cultures showed a rapid decrease of VCCs after reaching the maximum VCC, while all CSPR-cultures maintained stable VCCs throughout the cultivation. In particular, the culture targeting a stable CSPR of 20 pL $cell^{-1}$ d^{-1} maintained stable VCCs around 40×10^6 cells mL^{-1} with less than 10% variation and high viabilities (>90%) after day 2 and throughout the rest of cultivation. This observation could be an indicator for reaching a "steady-state" without intentional cell bleed, where the medium provided with a perfusion rate strategy targeting a CSPR of 20 pL $cell^{-1}$ d^{-1} supported the growth to cell densities around 40×10^6 cells mL^{-1}. This claim is supported by the stabilization of the metabolite profiles, where glucose and ammonium concentrations were maintained at constant levels with minimum fluctuations on day 5 and day 6. In contrast, lactate concentrations continued to decrease till day 8, which could indicate a shift of metabolism to lactate consumption, even though glucose was not depleted as reported in the literature by other studies (Altamirano et al., 2000, 2001, 2004; Dorai et al., 2009). However, more experiments with extended cultivation times are required to confirm the "steady-state" achieved without cell bleed. A concern was the accumulation of toxic by-products such as lactate and ammonium in the cell culture, with potentially detrimental effects due to decrease of pH by increasing lactate and impaired membrane transport by increased ammonium concentration (Hassell et al., 1991; Martinelle & Häggström, 1993). Overall, the results were comparable between partial and total medium exchanges for all CSPR-cultures investigated. Although lactate concentrations were initially lower for cultures with total medium exchanges, lactate concentrations of CSPR-cultures did not exceed values of 20 mmol L^{-1} above which toxic effects have been reported (Fu et al., 2016). Interestingly, the opposite was obtained for ammonium concentrations, which were lower throughout for all CSPR-cultures (<8 mmol L^{-1}) but remained below 10 mmol L^{-1} for both perfusion rate strategies and thus below values considered toxic for CHO cell culture (Hansen & Emborg, 1994; Lao & Toth, 1997). Thus, the decrease of VCC and viabilities for R1, low and medium CSPR-cultures cannot be explained by results obtained from metabolite measurements and might have been caused by the depletion or accumulation of unmeasured factors.

Although growth and metabolism were similar between perfusion rate strategies and with similar dynamics between inoculation

concentrations, slight differences were observed in the productivity results. The evaluation of the productivity focused on normalized values such as the cell-specific productivity and STY to allow comparison between different perfusion rate regimes (Bausch et al., 2019). For inoculation at CCD, the STY of R1 was threefold lower than STYs obtained for the culture targeting a stable CSPR of 20 pL cell^{-1} d^{-1}, whereas the opposite was found for inoculation at HCD, where the higher STYs were obtained for R1 and R2. Nonetheless, the endpoint STYs for R1 and high CSPR-cultures were very similar (within 5%). Furthermore, as a decrease of VCC was reported for R1 and R2 while the CSPR-culture targeting 20 pL cell^{-1} d^{-1} indicated stable growth, a beneficial effect of partial medium exchanges on productivity could potentially be present for extended cultivation times. For q_p values no significant difference at the 5% level could be seen at CCD inoculation, however between the low CSPR-cultures and R1 a p value of 0.052 was obtained, indicating that a significant difference might occur for higher inoculation or prolonged cultivation times. This was confirmed by the results from HCD inoculation culture, where a significant difference between perfusion rate strategies was obtained for low and medium, but not for high, CSPR-cultures targeting 20 pL cell^{-1} d^{-1}. The results of q_p and STY obtained for cultures targeting a CSPR of 20 pL cell^{-1} d^{-1} were comparable and in close agreement with the results of R1 and R2. This suggested that, although growth was supported at all CSPR targets, productivities were impacted by lower CSPRs. This shows that low CSPRs do not necessarily result in improved productivities and this finding is in agreement with observations previously reported in the literature (Lin et al., 2017).

As the aim was to maintain stable CSPRs during the growth phase through applying a different perfusion rate, the analysis of the perfusion rate dynamic and actual CSPR gave further insights into the development of these methods. The perfusion rate variation was found to be as expected, where the increase and stabilization correspond to the dynamic of the VCC for inoculation at both CCD and HCD. The lower perfusion rate of CSPR-cultures also indicates the lower medium consumption for CSPR-cultures. The >50-fold increased CSPRs obtained for R1 cultures, compared to CSPR-cultures at CCD inoculation, are a clear indication of the overfeeding of the culture when using the perfusion rate strategy based on a fixed RV d^{-1}. While for inoculation at CCD the actual CSPR of CSPR-cultures showed fluctuation at the beginning of the culture, for HCD inoculation cultures the CSPR was stable throughout the cultivations. The fluctuations observed were most likely due to the small medium exchange volumes, which were manually handled. Such variations are expected to be lower when the strategy is implemented in an automated system like a robotic platform, where a liquid handling arm is less prone to day-to-day error.

4.2 | CSPR-based perfusion rate strategy integrated with cell bleed

Secondly, the CSPR-based perfusion rate strategy was combined with a cell bleed strategy, which was presented and evaluated in Part I. During this experimentation three different CSPR setpoints were targeted, where two CSPRs were already investigated in the cultivations targeting maximum growth and a third higher CSPR was included. As observed before, all cultures showed very similar dynamics regarding growth and metabolism regardless of the perfusion rate strategy applied. The concentrations of key metabolites (glucose, lactate, and ammonium) were very stable throughout the cultivation, with minimal variations of 5% from the mean, where both lactate and ammonium remained well below concentrations considered toxic to the cells.

Although the dynamic profile of metabolites was comparable, cell growth seemed to have slowed down for CSPR-based cultures, showing an increased variability from day to day. This had an impact on the bleed rate which showed higher fluctuations when compared to the culture using the RV d^{-1}-based perfusion rate strategy. The slower growth could have been caused by the accumulation or near depletion of other metabolites which were not measured due to the limited working and sampling volumes. Furthermore, the analysis of the actual CSPR showed that the targets were not stable for all CSPR-cultures and in some cases remained lower than intended, which could also have influenced the growth dynamics. It is postulated that the manual handling of both the cell bleed (removal of cell suspension) and the partial medium exchange (removal of supernatant and addition of fresh medium) carried out post centrifugation were the likely sources of error and disturbed the cell culture. Care must be taken when the method is transferred to an automated platform to avoid such disturbances and ensure minimal impact of additions/removals from the bulk volume.

Nonetheless, the analysis of productivity results showed good agreement for both cell-specific productivity and STYs. This could be an indicator that even though cell growth was slowed down, the productivity was not negatively impacted. As the viabilities remain above 90% throughout the cultivation period, it could be interesting to investigate these conditions with a prolonged cultivation time to obtain more information about the impact of slower growth on the productivity, as slow cell growth and induced cell arrest were previously shown to result in high productivities (Ducommun et al., 2002; Gagnon et al., 2018; Wang et al., 2018).

5 | CONCLUSION

In this study, the successful application of two different perfusion rate strategies in an MWP at ultra-low working volumes of 1.2 mL was presented. HCD was achieved and maintained using both perfusion rate strategies. The comparison showed similar results regarding growth and productivities while the medium consumption was reduced by up to 50% for HCD cultures, when using the CSPR-based strategy. Having established the feasibility of evaluating different perfusion rate strategies in MWPs, such a system could be envisaged as a tool for cell clone screening and process development (e.g., CSPR screenings). A possible scenario would be to test leading clone candidates with perfusion rates targeting

multiple fixed CSPRs and evaluating cell growth and productivity for each case. Another scenario could use the method for a combination of media and process development studies, where different media compositions are tested at different CSPRs to obtain the best composition that supports the cell culture at minimal media usage to ensure cost efficiency. Subsequently, the most promising candidates could be transferred to small-scale models such as DWPs, ambr15® or larger small-scale perfusion bioreactors, such as the ambr250®, for in-depth analysis and fine-tuning. Further bioreactor operations are subject of future work which will also focus on the feasibility of this approach, for example with parallel investigations of multiple cell clones at several CSPR targets in a small-scale model, followed by transfer of the most promising candidates and CSPRs to mL-scale bioreactor for further analysis.

AUTHOR CONTRIBUTIONS

Marie Dorn: Conceptualization; methodology; formal analysis; investigation; data curation; writing—original draft preparation; writing—review and editing; visualization. **Ciara Lucas**: Data curation; writing—review and editing. **Kerensa Klottrup-Rees**: Writing—review and editing; supervision. **Ken Lee**: Writing—review and editing. **Martina Micheletti**: Conceptualization; resources; writing—review and editing; project administration; funding acquisition. All authors have read and agreed to the published version of the manuscript.

ACKNOWLEDGMENTS

The authors acknowledge Diane Hatton and Suzy Farid for their assistance in reviewing the manuscript. This study was supported by the UK Engineering and Physical Sciences Research Council (EPSRC) and AstraZeneca for the Engineering Doctorate studentship for Marie Dorn is gratefully acknowledged (Grant Ref: EP/S021868/1). This research is associated with the joint UCL-AstraZeneca Centre of Excellence for predictive decision-support tools in the bioprocessing sector and is aligned with the EPSRC Future Targeted Healthcare Manufacturing Hub hosted by UCL Biochemical Engineering.

CONFLICT OF INTEREST STATEMENT

The authors declare no conflict of interest.

DATA AVAILABILITY STATEMENT

The data that support the findings of this study are available upon reasonable request from the corresponding author, Martina Micheletti.

ORCID

Marie Dorn http://orcid.org/0000-0002-5188-258X
Ciara Lucas http://orcid.org/0000-0002-7027-8628
Martina Micheletti http://orcid.org/0000-0001-5147-0182

REFERENCES

Altamirano, C., Illanes, A., Casablancas, A., Gamez, X., Cairo, J. J., & Godia, C. (2001). Analysis of CHO cells metabolic redistribution in a glutamate-based defined medium in continuous culture. *Biotechnology Progress*, *17*(6), 1032–1041. https://doi.org/10.1021/bp0100981

Altamirano, C., Paredes, C., Cairó, J. J., & Gòdia, F. (2000). Improvement of CHO cell culture medium formulation: Simultaneous substitution of glucose and glutamine. *Biotechnology Progress*, *16*(1), 69–75. https://doi.org/10.1021/bp990124j

Altamirano, C., Paredes, C., Illanes, A., Cairó, J. J., & Gòdia, F. (2004). Strategies for fed-batch cultivation of t-PA producing CHO cells: Substitution of glucose and glutamine and rational design of culture medium. *Journal of Biotechnology*, *110*(2), 171–179. https://doi.org/10.1016/j.jbiotec.2004.02.004

Bausch, M., Schultheiss, C., & Sieck, J. B. (2019). Recommendations for comparison of productivity between fed-batch and perfusion processes. *Biotechnology Journal*, *14*(2), 1700721. https://doi.org/10.1002/biot.201700721

Chotteau, V. (2015). Perfusion processes. In M. Al-Rubeai (Ed.), *Animal cell culture* (Vol. 9, pp. 407–443). Springer.

Coolbaugh, M. J., Varner, C. T., Vetter, T. A., Davenport, E. K., Bouchard, B., Fiadeiro, M., Tugcu, N., Walther, J., Patil, R., & Brower, K. (2021). Pilot-scale demonstration of an end-to-end integrated and continuous biomanufacturing process. *Biotechnology and Bioengineering*, *118*(9), 3287–3301. https://doi.org/10.1002/bit.27670

Dorai, H., Kyung, Y. S., Ellis, D., Kinney, C., Lin, C., Jan, D., Moore, G., & Betenbaugh, M. J. (2009). Expression of anti-apoptosis genes alters lactate metabolism of Chinese hamster ovary cells in culture. *Biotechnology and Bioengineering*, *103*(3), 592–608. https://doi.org/10.1002/bit.22269

Dowd, J. E., Jubb, A., Kwok, K. E., & Piret, J. M. (2003). Optimization and control of perfusion cultures using a viable cell probe and cell specific perfusion rates. *Cytotechnology*, *42*(1), 35–45. https://doi.org/10.1023/A:1026192228471

Ducommun, P., Ruffieux, P. A., Kadouri, A., Von Stockar, U., & Marison, I. W. (2002). Monitoring of temperature effects on animal cell metabolism in a packed bed process. *Biotechnology and Bioengineering*, *77*(7), 838–842. https://doi.org/10.1002/bit.10185

Fu, T., Zhang, C., Jing, Y., Jiang, C., Li, Z., Wang, S., Ma, K., Zhang, D., Hou, S., Dai, J., Kou, G., & Wang, H. (2016). Regulation of cell growth and apoptosis through lactate dehydrogenase C over-expression in Chinese hamster ovary cells. *Applied Microbiology and Biotechnology*, *100*(11), 5007–5016. https://doi.org/10.1007/s00253-016-7348-4

Gagnon, M., Nagre, S., Wang, W., & Hiller, G. W. (2018). Shift to high-intensity, low-volume perfusion cell culture enabling a continuous, integrated bioprocess. *Biotechnology Progress*, *34*(6), 1472–1481. https://doi.org/10.1002/btpr.2723

Gränicher, G., Tapia, F., Behrendt, I., Jordan, I., Genzel, Y., & Reichl, U. (2021). Production of modified vaccinia Ankara virus by intensified cell cultures: A comparison of platform technologies for viral vector production. *Biotechnology Journal*, *16*(1), e2000024. https://doi.org/10.1002/biot.202000024

Hansen, H. A., & Emborg, C. (1994). Influence of ammonium on growth, metabolism, and productivity of a continuous suspension Chinese hamster ovary cell culture. *Biotechnology Progress*, *10*(1), 121–124. https://doi.org/10.1021/bp00025a014

Hassell, T., Gleave, S., & Butler, M. (1991). Growth inhibition in animal cell culture. *Applied Biochemistry and Biotechnology*, *30*(1), 29–41. https://doi.org/10.1007/bf02922022

Karst, D. J., Steinebach, F., Soos, M., & Morbidelli, M. (2017). Process performance and product quality in an integrated continuous antibody production process. *Biotechnology and Bioengineering*, *114*(2), 298–307. https://doi.org/10.1002/bit.26069

Konstantinov, K., Goudar, C., Ng, M., Meneses, R., Thrift, J., Chuppa, S., Matanguihan, C., Michaels, J., & Naveh, D. (2006). The 'push-to-low' approach for optimization of high-density perfusion cultures of animal cells. *Advances in Biochemical Engineering/Biotechnology*, *101*, 75–98. https://doi.org/10.1007/10_016

Lao, M. S., & Toth, D. (1997). Effects of ammonium and lactate on growth and metabolism of a recombinant Chinese hamster ovary cell

culture. *Biotechnology Progress*, *13*(5), 688–691. https://doi.org/10.1021/bp9602360

Lin, H., Leighty, R. W., Godfrey, S., & Wang, S. B. (2017). Principles and approach to developing mammalian cell culture media for high cell density perfusion process leveraging established fed-batch media. *Biotechnology Progress*, *33*(4), 891–901. https://doi.org/10.1002/btpr.2472

Lindstrom, S., & Andersson-Svahn, H. (2012). Single-cell culture in microwells. *Methods in Molecular Biology*, *853*, 41–52. https://doi.org/10.1007/978-1-61779-567-1_5

Martinelle, K., & Häggström, L. (1993). Mechanisms of ammonia and ammonium ion toxicity in animal cells: Transport across cell membranes. *Journal of Biotechnology*, *30*(3), 339–350. https://doi.org/10.1016/0168-1656(93)90148-G

Mayrhofer, P., Castan, A., & Kunert, R. (2021). Shake tube perfusion cell cultures are suitable tools for the prediction of limiting substrate, CSPR, bleeding strategy, growth and productivity behavior. *Journal of Chemical Technology & Biotechnology*, *96*(10), 2930–2939. https://doi.org/10.1002/jctb.6848

Nikolay, A., Bissinger, T., Granicher, G., Wu, Y., Genzel, Y., & Reichl, U. (2020). Perfusion control for high cell density cultivation and viral vaccine production. *Methods in Molecular Biology*, *2095*, 141–168. https://doi.org/10.1007/978-1-0716-0191-4_9

Ozturk, S. S. (1996). Engineering challenges in high density cell culture systems. *Cytotechnology*, *22*(1–3), 3–16. https://doi.org/10.1007/BF00353919

Schwarz, H., Gomis-Fons, J., Isaksson, M., Scheffel, J., Andersson, N., Andersson, A., Castan, A., Solbrand, A., Hober, S., Nilsson, B., & Chotteau, V. (2022). Integrated continuous biomanufacturing on pilot scale for acid-sensitive monoclonal antibodies. *Biotechnology and Bioengineering*, *119*(8), 2152–2166. https://doi.org/10.1002/bit.28120

Tregidgo, M., Lucas, C., Dorn, M., & Micheletti, M. (2023). Development of mL-scale pseudo-perfusion methodologies for high-throughput early phase development studies. *Biochemical Engineering Journal*, *195*, 108906. https://doi.org/10.1016/j.bej.2023.108906

Vázquez-Ramírez, D., Genzel, Y., Jordan, I., Sandig, V., & Reichl, U. (2018). High-cell-density cultivations to increase MVA virus production. *Vaccine*, *36*(22), 3124–3133. https://doi.org/10.1016/j.vaccine.2017.10.112

Villiger-Oberbek, A., Yang, Y., Zhou, W., & Yang, J. (2015). Development and application of a high-throughput platform for perfusion-based cell culture processes. *Journal of Biotechnology*, *212*, 21–29. https://doi.org/10.1016/j.jbiotec.2015.06.428

Wang, B., Albanetti, T., Miro-Quesada, G., Flack, L., Li, L., Klover, J., Burson, K., Evans, K., Ivory, W., Bowen, M., Schoner, R., & Hawley-Nelson, P. (2018). High-throughput screening of antibody-expressing CHO clones using an automated shaken deep-well system. *Biotechnology Progress*, *34*(6), 1460–1471. https://doi.org/10.1002/btpr.2721

Warikoo, V., Godawat, R., Brower, K., Jain, S., Cummings, D., Simons, E., Johnson, T., Walther, J., Yu, M., Wright, B., McLarty, J., Karey, K. P., Hwang, C., Zhou, W., Riske, F., & Konstantinov, K. (2012). Integrated continuous production of recombinant therapeutic proteins. *Biotechnology and Bioengineering*, *109*(12), 3018–3029. https://doi.org/10.1002/bit.24584

Wolf, M. K. F., Lorenz, V., Karst, D. J., Souquet, J., Broly, H., & Morbidelli, M. (2018). Development of a shake tube-based scale-down model for perfusion cultures. *Biotechnology and Bioengineering*, *115*(11), 2703–2713. https://doi.org/10.1002/bit.26804

Wolf, M., & Morbidelli, M. (2020). Development of mammalian cell perfusion cultures at lab scale: From orbitally shaken tubes to benchtop bioreactors. *Methods in Molecular Biology*, *2095*, 125–140. https://doi.org/10.1007/978-1-0716-0191-4_8

How to cite this article: Dorn, M., Lucas, C., Klottrup-Rees, K., Lee, K., & Micheletti, M. (2024). Platform development for high-throughput optimization of perfusion processes—Part II: Variation of perfusion rate strategies in microwell plates. *Biotechnology and Bioengineering*, 1–15. https://doi.org/10.1002/bit.28685